Mutations in DNAH17, Encoding a Sperm-Specific Axonemal Outer Dynein Arm Heavy Chain, Cause Isolated Male Infertility Due to Asthenozoospermia

Marjorie Whitfield, Lucie Thomas, Emilie Bequignon, Alain Schmitt, Laurence Stouvenel, Guy Montantin, Sylvie Tissier, Philippe Duquesnoy, Bruno Copin, Sandra Chantot, et al.

Mutations in *DNAH17*, encoding a sperm-specific axonemal outer dynein arm heavy chain, cause isolated male infertility due to asthenozoospermia.

Marjorie Whitfield[1,2,3,14], Lucie Thomas[4,14], Emilie Bequignon[5,6], Alain Schmitt[1,2,3], Laurence Stouvenel[1,2,3], Guy Montantin[7], Sylvie Tissier[7], Philippe Duquesnoy[4], Bruno Copin[7], Sandra Chantot[7], Florence Dastot[7], Catherine Faucon[8], Anne Laure Barbotin[9,10], Anne Loyens[11], Jean-Pierre Siffroi[4,7], Jean-François Papon[12,13], Estelle Escudier[4,7], Serge Amselem[4,7], Valérie Mitchell[9,10,15], Aminata Touré[1,2,3,15*] and Marie Legendre[4,7,15].

[1] INSERM U1016, Institut Cochin, Paris 75014, France.

[2] Centre National de la Recherche Scientifique UMR8104, Paris 75014, France.

[3] Faculté de Médecine, Université Paris Descartes, Sorbonne Paris Cité, Paris 75014, France. [4] Sorbonne Université, Institut National de la Santé et de la Recherche Médicale (INSERM U933), Hôpital Trousseau, Paris 75012, France.

[5] Assistance Publique-Hôpitaux de Paris (AP-HP), Hôpital Henri Mondor et Centre Hospitalier Intercommunal de Créteil, service d'Oto-Rhino-Laryngologie et de Chirurgie cervico-faciale. [6] Institut National de la Santé et de la Recherche Médicale (INSERM U955), CNRS, ERL 7240, Université Paris-Est, Faculté de Médecine, Créteil, 94010, France.

[7] Assistance Publique-Hôpitaux de Paris (AP-HP), Département de Génétique Médicale, Hôpital Trousseau, Paris 75012, France.

[8] Centre Hospitalier Intercommunal de Créteil, Laboratoire de microscopie électronique, Service d'Anatomopathologie, Créteil, 94010, France.

[9] CHU Lille, Reproductive Biology -Spermiology CECOS Institute, Jeanne de Flandre Hospital, F-59000 Lille, France.

[10] EA4308: Gametogenesis and Gamete Quality, Lille University, F-59000 Lille, France.

[11] Jean-Pierre Aubert Research Center, Laboratory of Development and Plasticity of the Neuroendocrine Brain, Institut National de la Santé et de la Recherche Médicale (INSERM U1172), Lille University, F59000 Lille, France.

[12] Institut National de la Santé et de la Recherche Médicale (INSERM U955), CNRS, ERL 7240, Université Paris-Sud, Faculté de Médecine, Créteil, 94010, France.

[13] Assistance Publique-Hôpitaux de Paris (AP-HP), Service d'Oto-Rhino-Laryngologie et de Chirurgie cervico-faciale, Hôpital Bicêtre, Le Kremlin-Bicêtre, F-94275, France.

[14] These authors contributed equally to this work

[15] These authors contributed equally to this work

[*] Correspondence: aminata.toure@inserm.fr

Running title: *DNAH17* mutations in isolated male infertility

Abstract

Motile cilia and sperm flagella share an evolutionarily conserved axonemal structure. Their structural and/or functional defects are associated with primary ciliary dyskinesia (PCD), a genetic disease characterized by chronic respiratory-tract infections and in which most males are infertile due to asthenozoospermia. Among the well-characterized axonemal protein complexes, the outer dynein arms (ODAs), through ATPase activity of their heavy chains (HCs), play a major role for cilia and flagella beating. However, the contribution of the different HCs (γ–type: DNAH5, DNAH8 and β–type: DNAH9, DNAH11, DNAH17) in ODAs from both organelles is unknown. By analyzing five male individuals consulting for isolated infertility and displaying a loss of ODAs in their sperm cells but not in respiratory cells, we identified bi-allelic mutations in *DNAH17*. The isolated infertility phenotype prompted us to compare the protein composition of ODAs in the sperm and ciliary axonemes from control individuals. We show that DNAH17 and DNAH8 colocalize with α-Tubulin along the sperm axoneme, but not DNAH5, DNAH9 nor DNAH11, while the reverse picture is observed in respiratory cilia, thus explaining the phenotype restricted to sperm cells. We also demonstrate the loss of function associated with *DNAH17* mutations in two unrelated individuals by performing western blot and immunofluorescence analyses on sperm cells, which indicated the absence of DNAH17 and DNAH8, whereas DNAH2 and DNALI, two inner dynein arm components, were present. Overall, this study demonstrates that mutations in *DNAH17* are responsible for isolated male infertility, and provides information regarding ODA composition in human spermatozoa.

Key words: DNAH17, dynein, ODA, axoneme, cilia, sperm flagellum, PCD, male infertility

REPORT

The axoneme is a highly evolutionarily conserved structure, which corresponds to the microtubule-based cytoskeleton, notably found in motile cilia and sperm flagella. This structure comprises an intricate network of protein complexes, which sustains the canonical conformation of nine doublets of microtubules (A and B) circularly arranged around a central pair of singlet microtubules ("9+2" pattern)[1]. Among the well-characterized axonemal protein complexes, the outer and inner dynein arms (ODAs and IDAs, respectively) play a major role for the beating of both cilia and sperm flagella[2]. ODAs and IDAs are multiprotein ATPase complexes, which comprise heavy, intermediate and light chains, and are attached to the A-microtubule of each peripheral doublets[3; 4]. By anchoring to the B-microtubule of the adjacent doublet, ODAs and IDAs drive the sliding of the microtubule doublets and behave as indispensable molecular motors for beating of those organelles.

In humans, structural and functional anomalies of motile cilia lead to primary ciliary dyskinesia (PCD [MIM: 244400]), a rare autosomal recessive disease, characterized by chronic airway infections with bronchitis and rhinosinusitis, associated with situs inversus in half cases (i.e. Kartagener syndrome)[5; 6]. At the ultrastructural level, the most frequent ciliary defects encountered in PCD individuals concern the dynein arms (DAs), and principally the ODAs, as illustrated by the loss of ODAs or both ODAs and IDAs in about 70% of PCD individuals[7-9]. In human respiratory cells, ODAs are constituted of a globular head domain, which comprises β- and γ-type heavy chains (β-HCs, γ-HC). This globular domain is associated with an intermediate domain, which comprises DNAI1 (MIM: 604366) and DNAI2 (MIM: 605483) intermediate dynein chains. In addition, various light chains such as DNAL1 (MIM: 610062), DNAL4 (MIM: 610565), are associated to the complex together with a docking subunit, which anchors the ODAs to the microtubules[10; 11]. Based on their dynein HCs composition, two types of ODAs have been reported in human respiratory cells:

type 1 ODAs locate at the proximal part of the cilia and contain DNAH5 (γ-HC) (MIM: 603335) and DNAH11 (β-HC) (MIM: 603339), while type 2 ODAs locate at the distal part of the cilia and contain DNAH5 (γ-HC) and DNAH9 (β-HC) (MIM: 603330)[12; 13].

To date, most of the PCD-associated gene mutations affect the assembly, anchoring or structure of the DAs[6; 7]. As expected from the structural similarities between motile cilia and flagella, most males affected by PCD are infertile and display severe or total asthenozoospermia[14], defined by the reduction or the absence of motile sperm[15]. Consequently, although the sperm phenotype of PCD individuals is generally poorly investigated, many of the PCD associated genes have been linked to male infertility [16]. Hence mutations in genes encoding ODA components, such as *DNAH5*[12], *DNAI1*[17], *DNAI2*[18] and *DNAH9*[19] were suggested to induce male infertility. While motile cilia and sperm flagella definitely share a similar axonemal structure, those organelles might display some structural and/or protein content differences that could explain (i) why not all men with PCD have asthenozoospermia, and (ii) conversely, the existence of axonemal defects restricted to the sperm flagella. Here we report the identification of mutations in *DNAH17* (MIM: 610063), encoding an axonemal heavy chain of the ODAs specifically expressed in the sperm cells, which result in male infertility due to asthenozoospermia but not in PCD.

We analyzed five male individuals who consulted for primary infertility and were enrolled in procedures of assisted reproduction technologies at the hospital of Lille, in France (Centre Hospitalier Regional Universitaire de Lille). Individuals 18GM00285 (II-1 from family 1) and 18GM01926 (II-1 from family 4) originated from France, individuals 18GM01913 and 18GM01974 (II-3 and II-4, respectively from family 2 GM03354) were two siblings from Algeria and born to a consanguineous union, and individual 18GM01932 (II-4 from family 3) originated from Morocco and was born to a consanguineous union. (**Table 1**). All five individuals had a normal somatic karyotype (46, XY), normal genital organs

development, normal FSH and Testosterone levels but presented with asthenozoospermia, defined by less than 40% of motile sperm in the ejaculate[15]. In particular the progressive motility was highly impacted as no, or only very few, progressive sperm were observed (between 0 and 5%; normal value >32%) (**Table 1**). All but one individuals (18GM01932) showed a severe reduction of the number of spermatozoa with normal morphology, compared to the normal value (between 2 to 12%; normal value>23%). Detailed sperm analysis indicated an increased number of spermatozoa with short, absent, irregularly shaped and coiled flagella, compared to the known distribution of these anomalies in fertile control individuals[20] (**Table 1; Table S1**). The presence of such mosaic of sperm anomalies in asthenozoospermic individuals was thoroughly described in the past and correspond to a "short tails" phenotype [21-23], recently renamed "Multiple Morphological Anomalies of the sperm Flagellum" (MMAF)[24]. In addition to asthenozoospermia, which was a constant feature in all individuals, reduced sperm count or vitality were recorded for individuals 18GM00285 (II-1 from family 1), 18GM01913 and 18GM01974 (II-3 and II-4, respectively from family 2) (**Table 1**). Ultrastructure analysis of the spermatozoa was performed by transmission electron microscopy (TEM) for all five individuals. In keeping with descriptions of the so-called MMAF phenotype[21-25], we observed spermatozoa with abnormal mitochondrial sheath and cytoplasmic bags containing unassembled flagellar components, together with severe axonemal disorganization, as illustrated by the absence of the central pair (9+0 pattern) and outer microtubule doublets (**Figure 1**). In addition, on all analyzed axonemal transversal sections (including those with microtubules disorganization), the absence of the ODAs was reported **(Table 1)** (**Figures 1, 2**). Importantly, while the absence of ODAs is a well-established ciliary defect associated with PCD, none of the five individuals displayed respiratory symptoms, nor situs inversus, following clinical interrogations and examinations (**Table 2**). Furthermore, respiratory investigations (including thoracic and ear, nose and throat

(ENT) tomodensitometry, mucociliary clearance, and ciliary analysis), which were performed for both siblings from family GM03354 and the unrelated individual 18GM01932, clearly excluded cystic fibrosis and PCD (**Table 2**). Lastly, TEM analyses, completed on airway epithelial cells (AECs) collected by nasal brushing from individual 18GM01913 (II-3 from family 2, in figure 3) and the unrelated individual 18GM01932 (II-4 from family 3, in figure 3), showed a normal ultrastructure of the ciliary axoneme and most notably, the presence of the ODAs in cilia (**Figure 2**). Taken together, the above data led us to conclude that the five individuals displayed a non-PCD associated form of asthenozoospermia due to specific loss of the ODAs in the sperm cells only. We subsequently intended to identify the genetic causes responsible for this phenotype. To this end, a signed informed consent was first obtained from all individuals to be included in the study, according to the local protocols and the principles of the Declaration of Helsinki. The study is approved by the Institutional Review Board of the French Institute of medical research and health (CEEI-IRB: opinion number 15-259) and the Comité de Protection des Personnes CPP Ile de France III (record number CPP02748).

The search for gene mutations underlying the absence of ODAs was performed in the four probands: 18GM00285, 18GM01974, 18GM01932 and 18GM01926 (II-1 from family 1, II-4 from family 2, II-4 from family 3 and II-1 from family 4, respectively, in figure 3) by a targeted capture panel (SeqCap EZ Choice, Roche) and parallel sequencing on a MiSeq system (Illumina) with genomic DNA extracted from EDTA blood samples. The targeted panel analyzed the 40 genes so far associated with PCD, including the *DNAH5*, *DNAH11* and *DNAH9* genes associated with the absence of ODAs, and *DNAH1* (MIM: 603332), a gene which was associated with male infertility due to the absence of IDAs in the sperm cells. In addition, two-hundred and fifty candidate genes for PCD were also sequenced, including the 7 other axonemal dynein heavy chains: *DNAH2* (MIM: 603333), *DNAH3* (MIM: 603334), *DNAH6* (MIM: 603336), *DNAH7* (MIM: 610061), *DNAH8* (MIM: 603337), *DNAH10* (MIM:

605884), *DNAH12* (MIM: 603340), *DNAH14* (MIM: 603341), and *DNAH17*. The enrichment probes targeted coding and non-coding exons and their flanking intronic regions; large indels were searched by depth ratio analysis. Raw data was computed through two independent pipelines as previously described[26]. Confirmation and analysis in the relatives from the four families was performed by Sanger sequencing **(Figure 3A)**. We identified bi-allelic variants in *DNAH17*, a gene not previously associated with PCD, in three probands and one brother: 18GM00285 (II-1 from family 1), 18GM01913 and 18GM01974 (II-3 and II-4, respectively from family 2) and 18GM01932 (II-4 from family 3). In addition, a heterozygous in-frame duplication in *DNAH17* was identified in the proband 18GM01926 (II-1 from family 4). Importantly, all individuals born to consanguineous union were shown to carry the identified *DNAH17* variations in the homozygous state **(Figure 3A)**. *DNAH17* (Genbank NM_173628; Ensembl ENSG00000187775) is located on chromosome 17 and contains 81 exons (transcript NM_173628.3), predicting a 4462-amino-acid protein (NCBI: NP_775899.3; UniProtKB: DYH17_Human Q9UFH2). The DNAH17 protein comprises nine principal domains: the DHC N1 and N2 conserved domains located in the stem of the dynein heavy chains and six ATPase domains (namely "ATPase associated with diverse cellular activities" domain; AAA domain) arranged in a ring-shaped molecular motor, which couple ATP binding and hydrolysis to conformational changes; in addition, the microtubule-binding region (MT) contains a coiled-coil stalk with a globular tip that binds to the B-tubule of the peripheral microtubule doublets **(Figure 3B)**.

Individual 18GM00285 (II-1 from family 1, in figure 3) carried two heterozygous *DNAH17* pathogenic mutations leading to a premature stop codon: a two-nucleotide deletion, c.1293_1294del p.Tyr431* and a 19-nucleotide deletion, c.7994_8012del p.Gly2665Glufs*4. The c.1293_1294del mutation, referenced as rs767723684, was present at a very low prevalence in the general population: 8.741e-6 (2 out of 228,814 alleles in gnomAD). The

c.7994_8012del deletion was absent from the gnomAD database. Both mutations introduce a premature stop codon (positions 431 and 2665, respectively, in the 4462-amino acid DNAH17 protein sequence) and are therefore expected to induce nonsense-mediated mRNA decay that is likely to prevent protein production. The two siblings 18GM01913 and 18GM01974 from family 2 (II-3 and II-4, respectively, in figure 3) were found to be homozygous for the c.5486G>A p.Cys1829Tyr missense variation. DNA sample from their father was not available; their mother was heterozygous for the variant and their brother, who fathered two children naturally, did not carry the variant. The p.Cys1829Tyr variation is not described in gnomAD; it does not seem prone to alter splicing as it only slightly weakens the MaxEntScan score of the intron 35 acceptor splice site (10.76 versus 11.03 for normal site). Importantly, Cysteine 1829 is highly conserved throughout evolution and conserved in 12 out the 13 axonemal dyneins (**Figure S1**). This residue lies 18 amino-acids from the ATPase catalytic site of the AAA1 domain, which among the six AAA domains, is the only one that retained an ATP hydrolyze activity. Altogether these elements suggest that the p.Cys1829Tyr missense variation is likely to disrupt the stability and/or the function of the protein. Individual 18GM01932 (II-4 from family 3, in figure 3) was homozygous for a complex allele, with two distinct missense variations: c.[10496C>T;10784T>C] p.[Pro3499Leu;Leu3595Pro], located in the AAA5 domain. None of these variations are described in gnomAD and they do not create donor or acceptor splice sites (MaxEntScan tool). These two variations involve a proline residue, the most effective amino acid in disrupting regular secondary structure elements[27], and are thus expected to strongly alter the protein structure by occasioning anomalous presence or absence of a Proline residue in the protein sequence. In addition, Proline 3499 and Leucine 3595 are conserved and highly conserved, respectively, throughout evolution; Leu3595 is also conserved among the 13 axonemal dyneins (**Figure S1**). Lastly, individual 18GM01926 (II-1 from family 4, in figure 3) carried a heterozygous 12-nucleotide

in-frame duplication: c.10486_10497dup p.Val3496_Pro3499dup and no other molecular defect was identified. This variant, which is not reported in gnomAD, does not create any donor or acceptor splice site within exon 65 (MaxEntScan); it is predicted to introduce a motif (Valine-Leucine-Asparte-Proline) within the AAA5 domain, which may also alter the secondary structure of the region due to the introduction of a Proline residue. In total, this molecular screening led to the identification of five *DNAH17* bi-allelic variations, considered to be highly likely pathogenic, in four individuals, and one heterozygous probably pathogenic variant in the fifth individual. Given (i) the nature of the predicted encoded protein by *DNAH17*, (ii) the above *in silico* data supporting the pathogenicity of all variants identified in *DNAH17*, (iii) the familial segregation of the variants in family GM03354 and GM03364, and (iv) the absence of other predicted pathogenic variants in genes encoding known components of dynein arms or in genes expressed in testis and/or related to cilia/flagella, we focused the subsequent studies on *DNAH17*, which appeared as the best candidate to explain the isolated primary male infertility observed in the five individuals.

To date, very few data on ODA composition of mammalian spermatozoa have been reported in the literature. Therefore, we first intended to better define the expression profile of the established human genes encoding the ODA heavy chains, namely *DNAH5*, *DNAH8*, *DNAH9*, *DNAH11* and *DNAH17*. First, by comparing the distribution of ODA heavy chains in tissue expression databases (EMBL-EBI Expression Atlas), and performing quantitative RT-PCR analyses on human adult tissues (**Figure S2**), we observed that *DNAH8* and *DNAH17* were clearly expressed in the testis and less abundant in the lung, while *DNAH5*, *DNAH9* and *DNAH11* were the most abundant heavy chains detected in the lung. In order to distinguish between somatic and germline expression and to specify the stage of differentiation of the germ cells, we analyzed available quantitative single-cell RNA sequencing datasets from human adult testis (ReproGenomics Viewer)[28-30]. In keeping with the expression pattern of

the genes involved in spermiogenesis, *DNAH8* and *DNAH17* expression were plainly detected in the germ cells from early spermatocyte to late spermatid stage but not in the somatic cells (Leydig, Sertoli cells) (**Figure S3A**). *DNAH9* was also detected in the germ cells but with a shorter window of expression, as the onset was observed in late spermatocyte/early spermatid stage. In agreement with their tissue distribution profile, the expression level of *DNAH5* and *DNAH11* was very low in both somatic and germ cells lineages of the testis. We next analyzed quantitative proteomic data available in the literature, which indicated that DNAH8 and DNAH17 proteins were both categorically detectable in human sperm proteome analyses[31; 32], while their amount was found very low in human airway cilia proteome[33] (**Figure S3B**). Conversely, DNAH5, DNAH9 and DNAH11 were not significantly detected in human sperm flagellar proteome (or only with a limited number of unique peptides identified by mass spectrometry), whereas they were strongly detected in the human ciliary proteome, being even part of the most abundant ciliary proteins. Taken together, the above data indicate that *DNAH8*, *DNAH9* and *DNAH17* transcripts are expressed in the germ cells during spermiogenesis. However, only DNAH8 and DNAH17 proteins are detected by proteomic analysis in mature spermatozoa.

In order to further confirm these data, we analyzed the presence and location of all ODA heavy chains proteins in AECs and spermatozoa from control individuals by performing western blot and immunofluorescence analyses. By means of western blot using antibodies directed against DNAH5, DNAH8, DNAH9, DNAH11 and DNAH17, we first show that DNAH8 and 17 are detected at the expected molecular weights in sperm cells but not in AECs, while DNAH5, DNAH9 and DNAH11 proteins are only detected in AECs (**Figure 4A**). Next, by means of immunofluorescence with co-staining of the axoneme with anti α-Tubulin antibody, we confirm the above results. Hence as previously described in AECs[12; 13], DNAH5 was detected along the full length of the cilia, while DNAH9 and DNAH11 protein

distributions were restricted to the distal and proximal part of the cilia, respectively. Noteworthy, we observed that neither DNAH8 nor DNAH17 were detected in cilia from AECs obtained from controls (**Figure 4B**). The opposite pictures were observed in spermatozoa from control individuals, where only DNAH8 and DNAH17 could be co-detected with the α-Tubulin, along the sperm flagellum, with the exception of the terminal piece, which is known to lack complete axonemal structure (**Figure 4B; Figure S4; Figure S5**). Taken together, these data indicate that the sperm cells harbor a set of ODA heavy chains (i.e. DNAH8 and DNAH17), which is distinct from that found in respiratory ciliated cells (i.e. DNAH5, DNAH9 and DNAH11). Such distribution pattern is consistent with the absence of ODAs in individuals carrying *DNAH17* mutations, which we found restricted to the sperm cells.

To confirm the pathogenicity of the identified *DNAH17* mutations, we analyzed the sperm protein content of individuals 18GM01932 (II-4 from family 3, in figure 3) and 18GM01926 (II-1 from family 4, in figure 3). When performing western blot analysis on equal number of spermatozoa, the DNAH17 protein was almost undetectable in sperm from those two individuals who carry *DNAH17* mutations, while the DNAI1 protein was present, although slightly diminished, in comparison to controls (**Figure 5A**). The absence of DNAH17 protein in sperm from these two individuals was also confirmed by immunofluorescence studies, as the DNAH17 signal was absent all along the flagellum with only small dots observed in the proximal region of the flagellum, while α-Tubulin staining was readily detectable (**Figure 5B**). We next analyzed other components of ODAs and IDAs to better assess the impact of *DNAH17* mutations in axonemal protein complexes, structure and assembly. Immunofluorescence studies performed on sperm cells from individuals 18GM01932 (II-4 from family 3, in figure 3) and 18GM01926 (II-1 from family 4, in figure 3) indicated that the heavy chain DNAH8 was totally absent from the sperm axoneme, thus

further confirming the absence of ODAs shown by TEM (**Figure 6A**). As previously observed by western blot analysis (**Figure 5A)**, the DNAI1 protein, an intermediate chain of the ODAs, was detected by immunofluorescence, in sperm from individuals 18GM01932 (II-4 from family 3, in figure 3) and 18GM01926 (II-1 from family 4, in figure 3), but in reduced amount, suggesting that part of the ODA may subsist but not be detectable by TEM (**Figure S5A**). Importantly, DNAH2, and DNALI1, corresponding to a heavy and a light/intermediate chain of the IDA, respectively, were both clearly detected in sperm from both individuals (**Figure 6B; Figure S5B)**, indicating that the IDAs are not impacted by *DNAH17* mutations.

In conclusion, we identified mutations in *DNAH17*, which we demonstrate to be associated with a specific loss of the ODAs in the sperm cells and recessive male infertility but not PCD. Four of the mutations were identified in the homozygous state, and one in the heterozygous state. Western blot and immunofluorescence detection in sperm from individual 18GM01932, carrying the two homozygous missense mutations, p.Leu3595Pro and p.Pro3499Leu, showed the absence of DNAH17 protein compared to controls, strongly supporting that the mutations, which incriminate a Proline residue, alter DNAH17 protein stability. To date, no crystal structure from axonemal dynein heavy chain is available. In order to retrieve more information about the impact of some of the DNAH17 mutations we identified on conserved residues among dynein heavy chain proteins, we used the available crystal structure of the closest human cytoplasmic heavy chain, DYNC1H1 (MIM: 600112) (reference 5NUG in PDB). Figure S7 presents the crystal structure of DYNC1H1 with the location of the three equivalent amino-acids targeted by the p.Cys1829Tyr, p.Pro3499Leu and p.Leu3595Pro DNAH17 mutations. From this representation the Cys1829 residue (1888 in DYNC1H1) appears close to the ADP binding site, while the Proline 3499 (3647 in DYNC1H1) residue is located at the end of an alpha-helix with consequences of its substitution towards a Leucine residue difficult to be predicted. The Leu3595 residue (3745 in

DYNC1H1) is located within an alpha-helix and its mutation toward a Proline residue seems prone to alter this secondary structure (Figure S7). Taken together, this information retrieved from comparison with the crystal structure of the cytosolic DYNC1H1, supports the potential pathogenic effects of the p.Cys1829Tyr and p.Leu3595Pro mutations.

Importantly, while a second molecular defect was not identified in individual 18GM01926 (II-1 from family 4, in figure 3), the DNAH17 protein was barely detectable in sperm from this individual by western blot or immunofluorescence. The absence of DNAH17 protein in sperm from individual 18GM01926 could be explained by i.) a mutation in the non-coding regions by a second *DNAH17* allele, ii.) a mutation in *DNAH8* as herein, conversely, we show *DNAH17* mutations are associated with loss of both DNAH17 and DNAH8 proteins, or iii.) a dominant negative effect of the identified heterozygous *DNAH17* mutation. Unfortunately, DNA samples from parents of individual 18GM01926 were not available, preventing to directly test some of the above hypotheses. In addition, the limited quantity of biological samples from individual 18GM01926 did not allow us to perform RT-PCR analyses. Nevertheless, from our genetic analyses, we can formally exclude the hypothesis of mutations in *DNAH8* as no pathogenic variants were identified for individual 18GM01926, nor for other individuals reported in this study (Table S2). Considering that the mutation carried by individual 18GM01926, is an in-frame duplication of 4 amino acids, containing a Proline residue, it is possible that the mutated protein acts through a dominant negative effect; a modification of the secondary structure could induce instability and degradation of the mutated protein together with that of associated proteins (i.e. the wild-type DNAH17 protein encoded by the second allele and DNAH8 protein). This would imply homo/hetero dimérisation and/or physical interaction of DNAH8/17 proteins, but importantly a transmission of the mutation by the mother or a neo-mutation in the proband; unfortunately, as mentioned above, we could not test this hypothesis. Alternatively, the phenotype of

individual 18GM01926 and the absence of DNAH17 protein could be attributed to a deep intronic mutation or a deletion in the regulatory sequences of *DNAH17*, which was not evidenced by analyses of the coding and flanking splice site sequences. As to date, PCD-associated mutations in dynein genes were associated with an autosomal recessive mode of transmission, we much more favour this later hypothesis.

Taken together these genetic findings indicate the importance of DNAH17 in the composition of sperm ODAs, which is supported by its expression profile. Hence by characterizing ODA heavy chains expression profile, we propose a model, in which the sperm flagellum is composed of only one type of ODAs, containing DNAH8 (γ-HC) and DNAH17 (β-HC), which both localize all along the axoneme (**Figure 7**). In this model, we exclude any contribution of the ciliary DNAH5 (γ-HC) and DNAH11 (β-HC) proteins. Furthermore, no distal/proximal restricted localizations of DNAH8 nor DNAH17 protein were observed along the flagellum, in contrast to respiratory cilia[12; 13] (**Figure 7**). Surprisingly, *DNAH9* transcripts were highly detected in germ cells by single cell RNA sequencing[30] but the protein was not reported in mass spectrometry analyses, and we did not detect DNAH9 in human spermatozoa by immunofluorescence nor by western blot assays, in contrast to a previous report based on immunofluorescence[12]. Considering the high amounts of transcripts detected during the last stage of spermiogenesis, the DNAH9 (β-HC) protein might fulfill a transient function in the spermatid cells and the protein amount, if present in mature spermatozoa, might be very low.

While the loss of the ODAs in sperm cells from all individuals carrying mutations in *DNAH17* was highlighted by TEM analyses, we observed by western blot and immunofluorescence analyses that DNAH17 and DNAH8 proteins were both absent but not DNAI1, although its amount was found reduced. This suggests that the mutant DNAH17 proteins might not be assembled into the axoneme and could be eliminated in the residual bodies during spermiogenesis or subjected to degradation, if not properly folded. In any of

these two situations, DNAH8, the expected (γ-HC) associated chain within the globular domain of the ODA, obeys to the same fate. The presence of DNAI1 in sperm flagellum of individuals carrying mutations in *DNAH17*, suggests that the entirety of the ODAs may not be lost, and that the intermediate domain of the ODAs may succeed in being assembled or stabilized, in the absence of the heavy chains, as recently demonstrated in the case of *DNAH9* mutations[19].

To date, about 40 genes associated with PCD have been identified[7] and their mutations affect most often the dyneins themselves or the pre-assembly, addressing or anchoring of the arms. Hence mutations in *DNAH5*[34; 35], *DNAI1*[36], *DNAI2*[18], *DNAL1*[37], *ARMC4* (MIM: 615408)[38], *CCDC114* (MIM: 615038)[39; 40] and *CCDC151* (MIM: 615956)[41] were identified in several PCD individuals with an absence of ODAs. Mutations in *DNAH9* were also identified but do not affect all ODAs due to the restricted distribution of the DNAH9 protein to the distal part of the cilia, and result in a PCD phenotype with moderate symptoms[19; 42]. Finally, *DNAH11* mutations were associated with PCD without ultrastructural defects[43-45]. Although the sperm phenotypes were poorly investigated in these studies, mutations in some of the above dynein genes were also suggested to be responsible for male infertility (*DNAH5*[12], *DNAI1*[17], *DNAI2*[18] and *DNAH9*[19]). Herein we demonstrate that mutations in *DNAH17* are not associated with PCD but exclusively responsible for male infertility. So far, this situation was only described once in the literature, in the case of mutations in *DNAH1*, which encodes an IDA dynein HC[24; 46-48]. Similarly to what we observed in case of *DNAH17* mutations, previous work identified mutations in *DNAH1* that are associated with severe asthenozoospermia due to MMAF phenotype and loss of IDAs[24]. In both cases, the sperm-restricted phenotype is explainable by nearly specific or preferential gene expression in the testis and sperm cells precursors. Despite this highly preferential tissue distribution, it can be difficult to state that mutations in those genes result in isolated infertility, and to exclude a

mild PCD phenotype when no other functional and structural analyses are performed. Herein, our data are strongly supported by the TEM analyses of both sperm cells and respiratory cells of the individuals, together with clinical examinations, therefore allowing us to exclude a PCD phenotype. Based on the study of several cohorts from various ethnical origins, *DNAH1* accounts for one of the most frequent genetic causes of the MMAF phenotype[25; 49]. The outcome of assisted reproduction technology procedures (i.e. fertilization, pregnancy and delivery rates), which were carried out for individuals with *DNAH1* mutations was not reported to be affected compared to non-*DNAH1* mutated MMAF individuals[50]. Herein, we observed that among the five individuals carrying mutations in *DNAH17*, four individuals did not succeed in achieving pregnancy using intracytoplasmic sperm injection (ICSI) (Table 1), thus suggesting that *DNAH17* mutations could impede ICSI outcome. Further studies of MMAF individuals together with genotype/phenotype correlations, should provide an estimation of the prevalence of *DNAH17* mutations and a prognosis for ICSI outcome in case of *DNAH17* mutations.

Lastly and intriguingly, while in ciliated cells, the loss of dynein arms does not induce structural disorganization of the axoneme, in sperm cells, the loss of IDAs and ODAs (induced by *DNAH1* and *DNAH17*, respectively) was associated with a global and severe disorganization of the axonemal structure, as illustrated by the absence of microtubules doublets. The pathophysiological mechanisms underlying this sperm specific phenotype are not known but probably result from axonemal assembly and/or stability defects, and are in line with expected differences in the mode of assembly and organization of cilia and sperm flagella. This study therefore emphasizes that despite evolutionary conservation, the axoneme of mammalian cilia and sperm flagella, display specific sets of homologous proteins, which may, in addition, harbor specific properties to each organelle.

Overall, our study provides a comprehensive analysis of ODA heavy chains distribution in human spermatozoa and demonstrate the importance of DNAH17 (β-HC) in sperm flagellum structure and motility. We demonstrate that DNAH17 (β-HC) mutations are associated with a loss of ODAs and male infertility but not with PCD. Our results reinforce the importance of better characterizing PCD individuals regarding their fertility status. As shown in this study, the axoneme of respiratory cilia and sperm flagella is not strictly identical; this therefore precludes the generalization of infertility in male individuals who carry mutations associated with PCD. A particular attention should be given to the fertility status of PCD male individuals, which must be ascertained based on spermocytograms and exclusion of any female infertility component. Conversely, male individuals consulting for infertility ought to be specifically questioned in order to highlight possible respiratory phenotypes. In the future, such refined clinical procedures should help in improving our understanding of the genetic causes of male infertility, as an isolated disease or part of the PCD phenotypic continuum.

DESCRIPTION OF SUPPLEMENTAL DATA

Supplemental Data include 7 figures and 1 table.

ACKNOWLEDGEMENTS

We thank all the individuals and their families for their cooperation, as well as all the referring physicians and Denise Escalier for initial TEM analyses. This work was supported by the Institut National de la Santé et de la Recherche Médicale (INSERM), the Centre National de la Recherche Scientifique (CNRS), the Université Paris Descartes, the Université Pierre et Marie Curie, the French National Research Agency (Grant ANR MASFLAGELLA 14-CE15-0002-03), the Fondation pour la Recherche Médicale grant DEQ20120323689, RaDiCo funded by the French National Research Agency under the specific programme "Investments for the Future" (Cohort grant agreement ANR-10-COHO-0003), the Legs Poix grant from the Chancellerie des Universités of Sorbonne Université, and the BEAT-PCD COST action.

DISCLOSURE OF INTERESTS

The authors have no conflict of interest to declare

WEB RESSOURCES

The URLs for data presented here are as follows:

Clustal Omega software, http://www.ebi.ac.uk/Tools/msa/clustalo/

EMBL EBI Expression Atlas, http://www.ebi.ac.uk/gxa/home

GnomAD Browser, https://gnomad.broadinstitute.org/

Leiden Open Variation Database (LOVD), https://databases.lovd.nl/shared/variants

MaxEntScan, http://genes.mit.edu/burgelab/maxent/Xmaxentscan_scoreseq.html

Online Mendelian Inheritance in Man (OMIM), http://omim.org/

Panther, http://www.pantherdb.org/tools/index.jsp

PDB, https://www.rcsb.org/

Provean, http://provean.jcvi.org/index.php

Protein database (PDB), http://www.rcsb.org/pdb/static.do?p=file_formats/pdb/index.html

Pymol software, https://pymol.org/2/

ReproGenomics Viewer, http://rgv.genouest.org/app/#/

SMART, http://smart.embl-heidelberg.de/Uniprot, https://www.uniprot.org/

REFERENCES

1. Ishikawa, T. (2017). Axoneme Structure from Motile Cilia. Cold Spring Harb Perspect Biol 9.
2. King, S.M. (2016). Axonemal Dynein Arms. Cold Spring Harb Perspect Biol 8.
3. Viswanadha, R., Sale, W.S., and Porter, M.E. (2017). Ciliary Motility: Regulation of Axonemal Dynein Motors. Cold Spring Harb Perspect Biol 9.
4. Pazour, G.J., Agrin, N., Walker, B.L., and Witman, G.B. (2006). Identification of predicted human outer dynein arm genes: candidates for primary ciliary dyskinesia genes. J Med Genet 43, 62-73.
5. Bisgrove, B.W., and Yost, H.J. (2006). The roles of cilia in developmental disorders and disease. Development 133, 4131-4143.
6. Mitchison, H.M., and Valente, E.M. (2017). Motile and non-motile cilia in human pathology: from function to phenotypes. J Pathol 241, 294-309.
7. Lucas, J.S., Barbato, A., Collins, S.A., Goutaki, M., Behan, L., Caudri, D., Dell, S., Eber, E., Escudier, E., Hirst, R.A., et al. (2017). European Respiratory Society guidelines for the diagnosis of primary ciliary dyskinesia. Eur Respir J 49.
8. Papon, J.F., Coste, A., Roudot-Thoraval, F., Boucherat, M., Roger, G., Tamalet, A., Vojtek, A.M., Amselem, S., and Escudier, E. (2010). A 20-year experience of electron microscopy in the diagnosis of primary ciliary dyskinesia. Eur Respir J 35, 1057-1063.
9. Noone, P.G., Leigh, M.W., Sannuti, A., Minnix, S.L., Carson, J.L., Hazucha, M., Zariwala, M.A., and Knowles, M.R. (2004). Primary ciliary dyskinesia: diagnostic and phenotypic features. Am J Respir Crit Care Med 169, 459-467.
10. Nicastro, D., Schwartz, C., Pierson, J., Gaudette, R., Porter, M.E., and McIntosh, J.R. (2006). The molecular architecture of axonemes revealed by cryoelectron tomography. Science 313, 944-948.
11. Hom, E.F., Witman, G.B., Harris, E.H., Dutcher, S.K., Kamiya, R., Mitchell, D.R., Pazour, G.J., Porter, M.E., Sale, W.S., Wirschell, M., et al. (2011). A unified taxonomy for ciliary dyneins. Cytoskeleton 68, 555-565.
12. Fliegauf, M., Olbrich, H., Horvath, J., Wildhaber, J.H., Zariwala, M.A., Kennedy, M., Knowles, M.R., and Omran, H. (2005). Mislocalization of DNAH5 and DNAH9 in respiratory cells from patients with primary ciliary dyskinesia. Am J Respir Crit Care Med 171, 1343-1349.
13. Dougherty, G.W., Loges, N.T., Klinkenbusch, J.A., Olbrich, H., Pennekamp, P., Menchen, T., Raidt, J., Wallmeier, J., Werner, C., Westermann, C., et al. (2016). DNAH11 Localization in the Proximal Region of Respiratory Cilia Defines Distinct Outer Dynein Arm Complexes. American journal of respiratory cell and molecular biology 55, 213-224.
14. Shapiro, A.J., Zariwala, M.A., Ferkol, T., Davis, S.D., Sagel, S.D., Dell, S.D., Rosenfeld, M., Olivier, K.N., Milla, C., Daniel, S.J., et al. (2016). Diagnosis, monitoring, and

treatment of primary ciliary dyskinesia: PCD foundation consensus recommendations based on state of the art review. Pediatr Pulmonol 51, 115-132.
15. Cooper, T.G., Noonan, E., von Eckardstein, S., Auger, J., Baker, H.W., Behre, H.M., Haugen, T.B., Kruger, T., Wang, C., Mbizvo, M.T., et al. (2010). World Health Organization reference values for human semen characteristics. Human reproduction update 16, 231-245.
16. Vanaken, G.J., Bassinet, L., Boon, M., Mani, R., Honore, I., Papon, J.F., Cuppens, H., Jaspers, M., Lorent, N., Coste, A., et al. (2017). Infertility in an adult cohort with primary ciliary dyskinesia: phenotype-gene association. Eur Respir J 50.
17. Guichard, C., Harricane, M.C., Lafitte, J.J., Godard, P., Zaegel, M., Tack, V., Lalau, G., and Bouvagnet, P. (2001). Axonemal dynein intermediate-chain gene (DNAI1) mutations result in situs inversus and primary ciliary dyskinesia (Kartagener syndrome). Am J Hum Genet 68, 1030-1035.
18. Loges, N.T., Olbrich, H., Fenske, L., Mussaffi, H., Horvath, J., Fliegauf, M., Kuhl, H., Baktai, G., Peterffy, E., Chodhari, R., et al. (2008). DNAI2 mutations cause primary ciliary dyskinesia with defects in the outer dynein arm. Am J Hum Genet 83, 547-558.
19. Fassad, M.R., Shoemark, A., Legendre, M., Hirst, R.A., Koll, F., le Borgne, P., Louis, B., Daudvohra, F., Patel, M.P., Thomas, L., et al. (2018). Mutations in Outer Dynein Arm Heavy Chain DNAH9 Cause Motile Cilia Defects and Situs Inversus. Am J Hum Genet 103, 984-994.
20. Auger, J., Jouannet, P., and Eustache, F. (2016). Another look at human sperm morphology. Hum Reprod 31, 10-23.
21. Chemes, H.E., Brugo, S., Zanchetti, F., Carrere, C., and Lavieri, J.C. (1987). Dysplasia of the fibrous sheath: an ultrastructural defect of human spermatozoa associated with sperm immotility and primary sterility. Fertil Steril 48, 664-669.
22. Escalier, D., and Albert, M. (2006). New fibrous sheath anomaly in spermatozoa of men with consanguinity. Fertil Steril 86, 219 e211-219.
23. Escalier, D. (2006). Arrest of flagellum morphogenesis with fibrous sheath immaturity of human spermatozoa. Andrologia 38, 54-60.
24. Ben Khelifa, M., Coutton, C., Zouari, R., Karaouzene, T., Rendu, J., Bidart, M., Yassine, S., Pierre, V., Delaroche, J., Hennebicq, S., et al. (2014). Mutations in DNAH1, which encodes an inner arm heavy chain dynein, lead to male infertility from multiple morphological abnormalities of the sperm flagella. Am J Hum Genet 94, 95-104.
25. Nsota Mbango, J.-F., Coutton, C., Arnoult, C., Ray, P., and Toure, A. (in press). Genetic causes of male infertility: Snapshot on Morphological Abnormalities of the Sperm Flagellum. Basic and clinical andrology.
26. Jeanson, L., Thomas, L., Copin, B., Coste, A., Sermet-Gaudelus, I., Dastot-Le Moal, F., Duquesnoy, P., Montantin, G., Collot, N., Tissier, S., et al. (2016). Mutations in GAS8, a Gene Encoding a Nexin-Dynein Regulatory Complex Subunit, Cause Primary Ciliary Dyskinesia with Axonemal Disorganization. Hum Mutat 37, 776-785.
27. Krieger, F., Moglich, A., and Kiefhaber, T. (2005). Effect of proline and glycine residues on dynamics and barriers of loop formation in polypeptide chains. J Am Chem Soc 127, 3346-3352.
28. Darde, T.A., Lecluze, E., Lardenois, A., Stevant, I., Alary, N., Tuttelmann, F., Collin, O., Nef, S., Jegou, B., Rolland, A.D., et al. (2019). The ReproGenomics Viewer: a multi-omics and cross-species resource compatible with single-cell studies for the reproductive science community. Bioinformatics.
29. Darde, T.A., Sallou, O., Becker, E., Evrard, B., Monjeaud, C., Le Bras, Y., Jegou, B., Collin, O., Rolland, A.D., and Chalmel, F. (2015). The ReproGenomics Viewer: an

integrative cross-species toolbox for the reproductive science community. Nucleic Acids Res 43, W109-116.
30. Wang, M., Liu, X., Chang, G., Chen, Y., An, G., Yan, L., Gao, S., Xu, Y., Cui, Y., Dong, J., et al. (2018). Single-Cell RNA Sequencing Analysis Reveals Sequential Cell Fate Transition during Human Spermatogenesis. Cell Stem Cell 23, 599-614 e594.
31. Wang, G., Guo, Y., Zhou, T., Shi, X., Yu, J., Yang, Y., Wu, Y., Wang, J., Liu, M., Chen, X., et al. (2013). In-depth proteomic analysis of the human sperm reveals complex protein compositions. J Proteomics 79, 114-122.
32. Amaral, A., Castillo, J., Estanyol, J.M., Ballesca, J.L., Ramalho-Santos, J., and Oliva, R. (2013). Human sperm tail proteome suggests new endogenous metabolic pathways. Mol Cell Proteomics 12, 330-342.
33. Blackburn, K., Bustamante-Marin, X., Yin, W., Goshe, M.B., and Ostrowski, L.E. (2017). Quantitative Proteomic Analysis of Human Airway Cilia Identifies Previously Uncharacterized Proteins of High Abundance. J Proteome Res 16, 1579-1592.
34. Hornef, N., Olbrich, H., Horvath, J., Zariwala, M.A., Fliegauf, M., Loges, N.T., Wildhaber, J., Noone, P.G., Kennedy, M., Antonarakis, S.E., et al. (2006). DNAH5 mutations are a common cause of primary ciliary dyskinesia with outer dynein arm defects. Am J Respir Crit Care Med 174, 120-126.
35. Olbrich, H., Haffner, K., Kispert, A., Volkel, A., Volz, A., Sasmaz, G., Reinhardt, R., Hennig, S., Lehrach, H., Konietzko, N., et al. (2002). Mutations in DNAH5 cause primary ciliary dyskinesia and randomization of left-right asymmetry. Nat Genet 30, 143-144.
36. Pennarun, G., Escudier, E., Chapelin, C., Bridoux, A.M., Cacheux, V., Roger, G., Clement, A., Goossens, M., Amselem, S., and Duriez, B. (1999). Loss-of-function mutations in a human gene related to Chlamydomonas reinhardtii dynein IC78 result in primary ciliary dyskinesia. Am J Hum Genet 65, 1508-1519.
37. Mazor, M., Alkrinawi, S., Chalifa-Caspi, V., Manor, E., Sheffield, V.C., Aviram, M., and Parvari, R. (2011). Primary ciliary dyskinesia caused by homozygous mutation in DNAL1, encoding dynein light chain 1. Am J Hum Genet 88, 599-607.
38. Hjeij, R., Lindstrand, A., Francis, R., Zariwala, M.A., Liu, X., Li, Y., Damerla, R., Dougherty, G.W., Abouhamed, M., Olbrich, H., et al. (2013). ARMC4 mutations cause primary ciliary dyskinesia with randomization of left/right body asymmetry. Am J Hum Genet 93, 357-367.
39. Knowles, M.R., Leigh, M.W., Ostrowski, L.E., Huang, L., Carson, J.L., Hazucha, M.J., Yin, W., Berg, J.S., Davis, S.D., Dell, S.D., et al. (2013). Exome sequencing identifies mutations in CCDC114 as a cause of primary ciliary dyskinesia. Am J Hum Genet 92, 99-106.
40. Onoufriadis, A., Paff, T., Antony, D., Shoemark, A., Micha, D., Kuyt, B., Schmidts, M., Petridi, S., Dankert-Roelse, J.E., Haarman, E.G., et al. (2013). Splice-site mutations in the axonemal outer dynein arm docking complex gene CCDC114 cause primary ciliary dyskinesia. Am J Hum Genet 92, 88-98.
41. Hjeij, R., Onoufriadis, A., Watson, C.M., Slagle, C.E., Klena, N.T., Dougherty, G.W., Kurkowiak, M., Loges, N.T., Diggle, C.P., Morante, N.F., et al. (2014). CCDC151 mutations cause primary ciliary dyskinesia by disruption of the outer dynein arm docking complex formation. Am J Hum Genet 95, 257-274.
42. Loges, N.T., Antony, D., Maver, A., Deardorff, M.A., Gulec, E.Y., Gezdirici, A., Nothe-Menchen, T., Hoben, I.M., Jelten, L., Frank, D., et al. (2018). Recessive DNAH9 Loss-of-Function Mutations Cause Laterality Defects and Subtle Respiratory Ciliary-Beating Defects. Am J Hum Genet 103, 995-1008.

43. Bartoloni, L., Blouin, J.L., Pan, Y., Gehrig, C., Maiti, A.K., Scamuffa, N., Rossier, C., Jorissen, M., Armengot, M., Meeks, M., et al. (2002). Mutations in the DNAH11 (axonemal heavy chain dynein type 11) gene cause one form of situs inversus totalis and most likely primary ciliary dyskinesia. Proc Natl Acad Sci U S A 99, 10282-10286.
44. Schwabe, G.C., Hoffmann, K., Loges, N.T., Birker, D., Rossier, C., de Santi, M.M., Olbrich, H., Fliegauf, M., Failly, M., Liebers, U., et al. (2008). Primary ciliary dyskinesia associated with normal axoneme ultrastructure is caused by DNAH11 mutations. Hum Mutat 29, 289-298.
45. Knowles, M.R., Leigh, M.W., Carson, J.L., Davis, S.D., Dell, S.D., Ferkol, T.W., Olivier, K.N., Sagel, S.D., Rosenfeld, M., Burns, K.A., et al. (2012). Mutations of DNAH11 in patients with primary ciliary dyskinesia with normal ciliary ultrastructure. Thorax 67, 433-441.
46. Amiri-Yekta, A., Coutton, C., Kherraf, Z.E., Karaouzene, T., Le Tanno, P., Sanati, M.H., Sabbaghian, M., Almadani, N., Sadighi Gilani, M.A., Hosseini, S.H., et al. (2016). Whole-exome sequencing of familial cases of multiple morphological abnormalities of the sperm flagella (MMAF) reveals new DNAH1 mutations. Hum Reprod 31, 2872-2880.
47. Sha, Y., Yang, X., Mei, L., Ji, Z., Wang, X., Ding, L., Li, P., and Yang, S. (2017). DNAH1 gene mutations and their potential association with dysplasia of the sperm fibrous sheath and infertility in the Han Chinese population. Fertil Steril 107, 1312-1318 e1312.
48. Wang, X., Jin, H., Han, F., Cui, Y., Chen, J., Yang, C., Zhu, P., Wang, W., Jiao, G., Wang, W., et al. (2017). Homozygous DNAH1 frameshift mutation causes multiple morphological anomalies of the sperm flagella in Chinese. Clin Genet 91, 313-321.
49. Coutton, C., Martinez, G., Kherraf, Z.E., Amiri-Yekta, A., Boguenet, M., Saut, A., He, X., Zhang, F., Cristou-Kent, M., Escoffier, J., et al. (2019). Bi-allelic Mutations in ARMC2 Lead to Severe Astheno-Teratozoospermia Due to Sperm Flagellum Malformations in Humans and Mice. Am J Hum Genet 104, 331-340.
50. Wambergue, C., Zouari, R., Fourati Ben Mustapha, S., Martinez, G., Devillard, F., Hennebicq, S., Satre, V., Brouillet, S., Halouani, L., Marrakchi, O., et al. (2016). Patients with multiple morphological abnormalities of the sperm flagella due to DNAH1 mutations have a good prognosis following intracytoplasmic sperm injection. Hum Reprod 31, 1164-1172.
51. Lhuillier, P., Rode, B., Escalier, D., Lores, P., Dirami, T., Bienvenu, T., Gacon, G., Dulioust, E., and Toure, A. (2009). Absence of annulus in human asthenozoospermia: case report. Human reproduction 24, 1296-1303.
52. Tamalet, A., Clement, A., Roudot-Thoraval, F., Desmarquest, P., Roger, G., Boule, M., Millepied, M.C., Baculard, T.A., and Escudier, E. (2001). Abnormal central complex is a marker of severity in the presence of partial ciliary defect. Pediatrics 108, E86.

FIGURE LEGENDS

Figure 1. **TEM analysis of spermatozoa from individuals 18GM01913, 18GM01932 and 18GM01926 with a MMAF phenotype**

(**A**) Left: longitudinal section of control spermatozoa with the head, comprising the nucleus (N) and acrosome (Ac). The flagellum extends from the head and comprises the axoneme (Ax), which is surrounded by mitochondria (M) in the midpiece and the fibrous sheath (FS) in the principal piece. Right inset: transversal section of control spermatozoa in the principal piece region. The axoneme comprises 9 doublets of microtubules (MTD) circularly arranged around a central pair (CP) of microtubules. A few other peri-axonemal structures, such as the outer dense fibers (ODF) and the longitudinal columns (LC), are visible. (**B, C**) Longitudinal sections of spermatozoa from individuals 18GM01913 (II-3 from family 2, in figure 3), 18GM01932 (II-4 from family 3, in figure 3) showing cytoplasmic bags with unassembled axonemal and peri-axonemal components, in due place of the flagellum. (**D, E**) Transversal sections of spermatozoa from individuals 18GM01926 (II-1 from family 4, in figure 3), 18GM01932 (II-4 from family 3, in figure 3), showing the lack of the central pair (9+0 pattern) and the lack of outer microtubules doublets. Scale bars: 2μm (A, B, C); 50 nm (D, E). Human sperm cells were processed for TEM analysis as previously described[51].

Figure 2. Comparative TEM analysis of spermatozoa and airway cilia from individuals 18GM01913, 18GM01926 and 18GM01932.

Upper panel: spermatozoa from a control individual and from individuals 18GM01926 (II-1 from family 4, in figure 3) and 18GM01932 (II-4 from family 3, in figure 3). (**A, C**) Axonemal sections from the sperm midpiece, showing mitochondria and outer dense fibers (ODF). Outer dynein arms (ODAs) are indicated by white arrow heads in the control and are absent in individual 18GM01926 (II-1 from family 4, in figure 3). (**B, D**) Axonemal sections

from the sperm principal piece. Outer dynein arms (ODAs) are indicated by arrow heads in the control and are absent in individual 18GM01932. **Lower panel**: Cilia from airway epithelial cells (AECs) from individuals 18GM01913 (II-3 from family 2, in figure 3) and 18GM01932. (**E, F**) Axonemal sections from AECs cilia showing the presence of ODAs, indicated by arrow heads. Scale bars: upper panel 100 nm (A, C), 50 nm (B, D); lower panel: 50 nm (E, F). Human sperm cells and nasal biopsy were processed for TEM analysis as previously described[51; 52].

Figure 3. Identification of *DNAH17* mutations in five infertile males from four unrelated families.

(**A**) Pedigree of the four unrelated families and Sanger sequencing data of the mutations identified in infertile individuals (solid symbols): 18GM00285 (II-1 from family 1), 18GM01913 and 18GM01974 (II-3 and II-4, respectively, from family 2), 18GM01932 (II-4 from family 3) and 18GM01926 (II-1 from family 4). The double line indicates consanguinity between parents. (**B**) Schematic representation of *DNAH17* exons structure (top) and predicted protein domains (bottom), according to SMART webtool and Uniprot, with position of the six different mutations identified in the five infertile individuals. All mutations are declared and accessible in LOVD public variation database with the following identification numbers: 0000473833 (c.1293_1294del p.Tyr431*); 0000473834 (c.7994_8012del p.Gly2665Glufs*4); 0000473835 (c.5486G>A p.Cys1829Tyr); 0000473837 (c.10496C>T p.Pro3499Leu) ; 0000473838 (c.10784T>C p.Leu3595Pro) ; 0000473840(c.10486_10497dup p.Val3496_Pro3499dup). DHC N1 and N2 (blue boxes) are conserved domains in the stem of dynein heavy chains. AAA1 to AAA6 (green boxes) indicate ATPases domains (ATPase associated with diverse cellular activities, AAA), arranged in a ring-shaped molecular motor, which couple ATP binding and hydrolysis to conformational changes. The microtubule-

binding region (MT, red box) is made of a coiled-coil stalk with a globular tip that binds to the adjacent B microtubule.

Figure 4. ODA HC proteins detection and localization in human sperm cells and AECs from healthy control individuals.

(**A**) Detection of DNAH8, DNAH9 and DNAH17 proteins by western blot in spermatozoa (Spz1, Spz2) and AECs (AEC1, AEC2) from two control individuals; DNAI1 was used for loading control. Airway epithelial cells and spermatozoa, obtained by nasal brushing and masturbation, respectively, were suspended in lysis buffer (50mM Tris, 150 mM NaCl, 1% Triton X-100, and Complete Protease Inhibitor Cocktail, Roche Diagnostics). Lysates were sonicated and cleared by centrifugation. Equal amounts of cells were loaded on 4-12% gradient SDS-PAGE and transferred overnight on a PVDF membrane. The primary antibodies (SIGMA DNAH8 HPA028447, DNAH9 HPA052641, DNAH17 HPA024354 and DNAI1 HPA021649) were incubated overnight at 4°C. Secondary antibody coupled to HRP (SIGMA rabbit HRP A0545) and Amersham ECL Select Western Blotting Detection Reagent were used for detection.

(**B**) Immunofluorescence staining of AECs and spermatozoa from a control with ODA heavy chain antibody (in red) and α-Tubulin (in green). Cells were counterstained with DAPI (blue) as nuclei marker. Scale bars represent 5µm. AECs obtained by airway brushing were cytocentrifugated onto glass slides and fixed 15 min with 4% paraformaldehyde. Spermatozoa were smeared onto glass slides and fixed 10 min with 4% paraformaldehyde followed by epitope retrieval in citrate buffer (pH 6). Cells were permeabilized in Triton X-100 for 10 min (0.1% for AECs, 0.2% for spermatozoa) and labeled with rabbit polyclonal antibody directed against ODA heavy chains DNAH5 (SIGMA HPA037470), DNAH8 (SIGMA HPA028447), DNAH9 (SIGMA HPA052641), DNAH11 (SIGMA HPA045880) and DNAH17 (SIGMA

HPA024354) and were co-stained with acetylated α-Tubulin (mouse monoclonal Abcam ab24610) for AECs and α-Tubulin (mouse monoclonal SIGMA DM1A T9026) for spermatozoa.

Figure 5. DNAH17 protein amount and localization in spermatozoa from 18GM01932 and 18GM01926 mutation carriers.

(**A**) Detection of DNAH17 protein by western blot in spermatozoa from two controls and from individuals 18GM01932 (II-4 from family 3, in figure 3) and 18GM01926 (II-1 from family 4, in figure 3). DNAI1 was used as positive control. Spermatozoa were suspended in lysis buffer (50mM Tris, 150mM NaCl, 1% Triton X-100, and complete protease inhibitor cocktail, Roche Diagnostics). Lysates were sonicated and cleared by centrifugation. The same amount of cells was loaded on a 4-12% gradient SDS-PAGE gel that was transferred overnight on a PVDF membrane. The membrane was incubated overnight at 4°C with primary antibodies (SIGMA DNAH17 HPA024354 and DNAI1 HPA021649). Following incubation with the secondary antibody (rabbit HRP SIGMA A0545), proteins were detected using Amersham ECL Select Western Blotting Detection Reagent.

(**B**) Immunofluorescence staining of spermatozoa from a control individual and from individuals 18GM01926 (II-1 from family 4, in figure 3) and18GM01932 (II-4 from family 3, in figure 3) with DNAH17 (in red) and α-Tubulin (in green). Spermatozoa were counterstained with DAPI (blue) as nuclei marker. Scale bars represent 5µm. Spermatozoa were smeared onto glass slides and fixed 10 min with 4% paraformaldehyde before epitope retrieval in citrate buffer pH 6. Spermatozoa were then permeabilized in Triton X-100, 0.2% 10 min and blocked 1 hour with 1% bovine serum albumin (BSA). Finally, cells were labeled with rabbit polyclonal antibody directed against DNAH17 (SIGMA HPA024354) and α-Tubulin (mouse monoclonal DM1A SIGMA T9026), followed by secondary antibody

incubation (anti-rabbit Alexa 568 and anti-mouse Alexa 488, Invitrogen) and mounting in DAPI Vectashield (Vector).

Figure 6. Immunostaining of DNAH8 and DNAH2 in spermatozoa from a healthy control and individuals 18GM01926 and 18GM01932.

(**A**) Immunofluorescence staining of spermatozoa from control and from individuals 18GM01926 (II-1 from family 4, in figure 3) and 18GM01932 (II-4 from family 3, in figure 3) with DNAH8 (γ-HC ODA, in red) and α-Tubulin (in green). (**B**) Immunofluorescence of spermatozoa from control and from individuals 18GM01926 (II-1 from family 4, in figure 3) and 18GM01932 (II-4 from family 3, in figure 3) with DNAH2 (a heavy chain of IDAs, in red) and α-Tubulin (in green). Spermatozoa were counterstained with DAPI (blue) as nuclei marker. Scale bars represent 5µm. Spermatozoa were smeared onto glass slides and fixed 10 min with 4% paraformaldehyde before epitope retrieval in citrate buffer pH 6. Spermatozoa were then permeabilized in Triton X-100, 0.2% 10 min and blocked 1 hour with 1% bovine serum albumin (BSA). Finally, cells were labeled with rabbit polyclonal antibody directed against DNAH8 (SIGMA HPA028447) or DNAH2 (SIGMA HPA067103) and α-Tubulin (mouse monoclonal DM1A SIGMA T9026), followed by secondary antibody incubation (anti-rabbit Alexa 568 and anti-mouse Alexa 488, Invitrogen) and mounting in DAPI Vectashield (Vector).

Figure 7. Schematic model of ODA heavy chains distribution in human AEC and sperm flagellum axonemes.

Longitudinal view of the axoneme from AEC cilia and sperm flagellum, illustrating ODA heavy chain composition. In respiratory cilia, γ-heavy chains are composed of DNAH5 (in orange), which locates along the full length of axoneme. The β-heavy chains (in blue) are

composed of DNAH11 (light blue) in the proximal part and DNAH9 (blue) in the distal part of the axoneme. In spermatozoa, we propose a model, in which ODAs are exclusively composed by the γ-HC DNAH8 and the β-HC DNAH17, which both localize all along the axoneme.

Table 1. Phenotypic features and semen characteristics of individuals with identified *DNAH17* mutations

						Semen Characteristics						Flagellar abnormalities					
Family (Origin)	Individuals	Known Consanguinity	Gender (Age)	Fertility	Sperm TEM	pH	Volume (ml)	Total sperm count (10^6)	Total Motility	Progressive Motility	Vitality	Absent	Short	Irregular Caliber	Coiled	Multiple	Typical forms
GM02359 (France/Italy)	18GM00285	no	male (36 y.)	Infertility[a]	ODA loss (100%)	8.1	2.5	**20**	**10**	**1**	72	5	**2**	**36**	**27**	1	**11**
GM03354 (Algeria)	18GM01974	yes	male (35 y.)	Infertility [a]	ODA loss (100%)	8	3.5	119	**1**	**0**	**51**	**12**	**34**	**16**	**38**	**2**	**2**
	18GM01913	yes	male (37 y.)	Infertility [a]	ODA loss (100%)	8	3.8	**27.7**	**1**	**0**	61	**16**	**34**	**14**	**38**	0	**4**
GM03364 (Morocco)	18GM01932	yes	male (27 y.)	Infertility [a]	ODA loss (100%)	7.8	4.5	88.6	**25**	**5**	76	2	1	**6**	**18**	**2**	22
GM03360 (France)	18GM01926	no	male (30 y.)	Infertility	ODA loss (100%)	7.7	6	198	**20**	**2**	60	2	**2**	**12**	**22**	0	**12**
Lower reference values for semen analysis						7.2	1.5	39	40	32	58	5	1	2	17	1	23

Values are percentages unless specified otherwise. Lower reference limits for semen analysis are provided, according to the World Health Organization (WHO) standards[15] and the distribution range of morphologically normal spermatozoa observed in 926 fertile individuals[20]. ([a]) ICSI failure (1-3 attempts); in bold characters: abnormal values.
Individual 18GM00285: II-1 from family 1; **Individuals 18GM01913 and 18GM01974**: II-3 and II-4, respectively, from family 2; **Individual 18GM01932**: II-4 from family 3; **Individual 18GM01926**: II-1 from family 4.

Table 2. Respiratory phenotypic features of individuals with identified *DNAH17* mutations

Individuals	Airway disease	SI	Cilia TEM	Other explorations
18GM00285	no	no	NA	NA
18GM01974	no	no	NA	normal thoracic/ENT TDM, normal mucociliary clearance
18GM01913	no	no	normal (ODA present)	normal thoracic/ENT TDM, normal mucociliary clearance
18GM01932	no	no	normal (ODA present)	normal ciliary beating, normal thoracic/ENT TDM, normal mucociliary clearance
18GM01926	no	no	NA	NA

SI: Situs Inversus, TEM: Transmission Electronic Microscopy, NA: not available, ENT: Ears, Nose and Throat, TDM: Tomodensitometry

Individuals 18GM00285: II-1 from family 1; 18GM01913: II-3 from family 2; 18GM01974: II-4 from family 2; 18GM01932: II-4 from family 3; 18GM01926: II-1 from family 4.

Figure 1

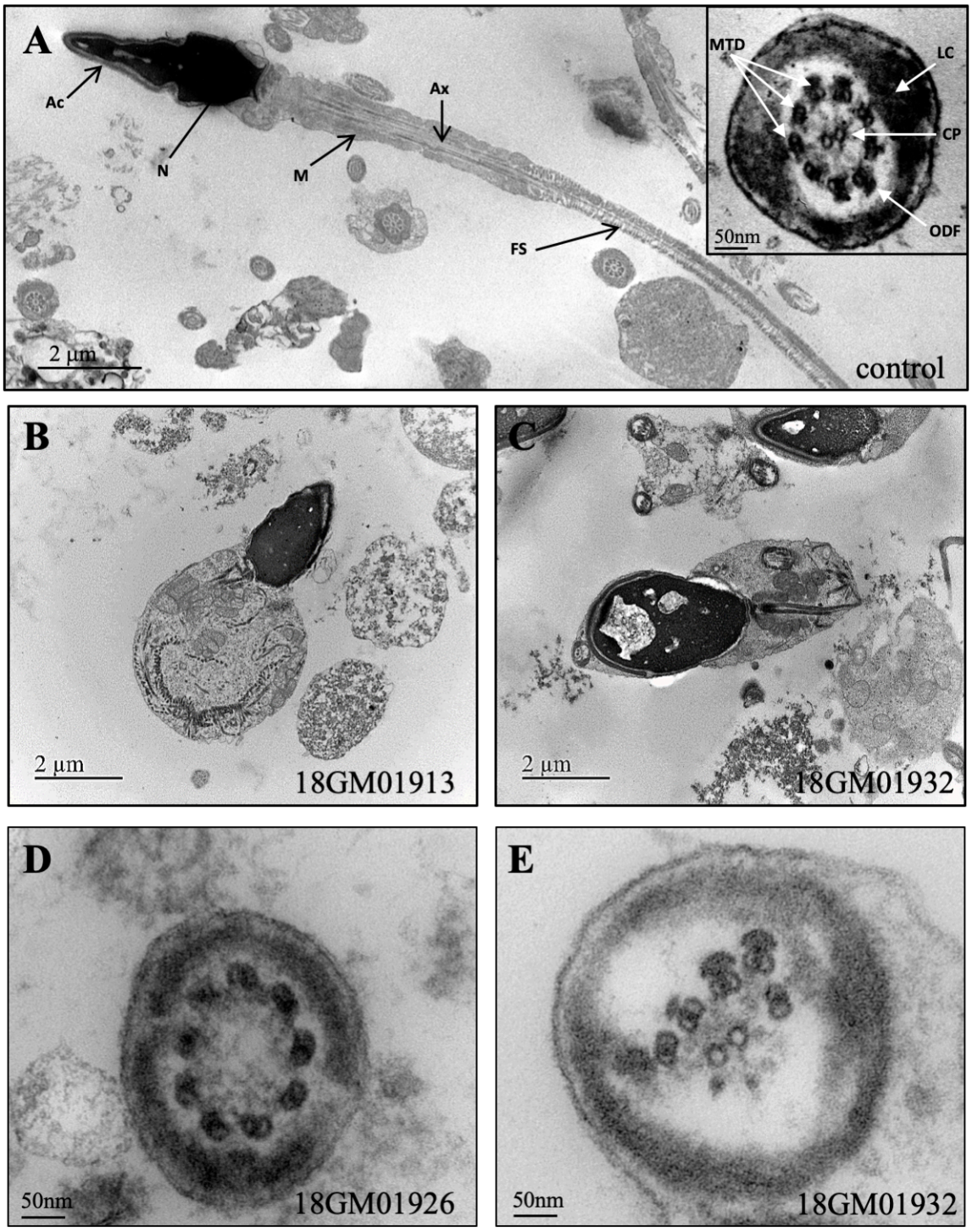
A
Ac
N
M
Ax
FS
2 μm
control
MTD
LC
CP
ODF
50nm
B
2 μm
18GM01913
C
2 μm
18GM01932
D
50nm
18GM01926
E
50nm
18GM01932

Figure 2

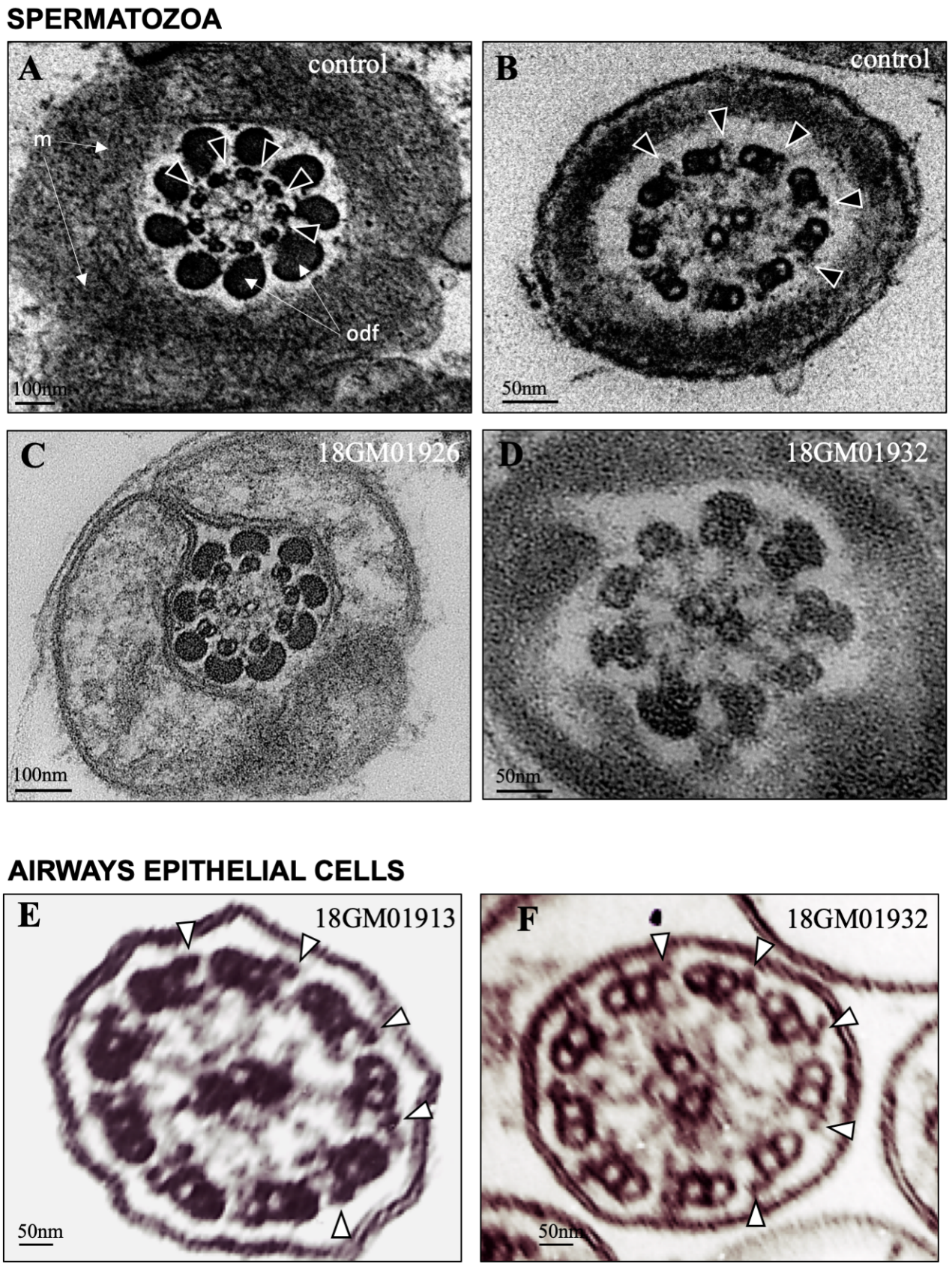
SPERMATOZOA
A
control
m
odf
100nm
B
control
50nm
C
18GM01926
100nm
D
18GM01932
50nm
AIRWAYS EPITHELIAL CELLS
E
18GM01913
50nm
F
18GM01932
50nm

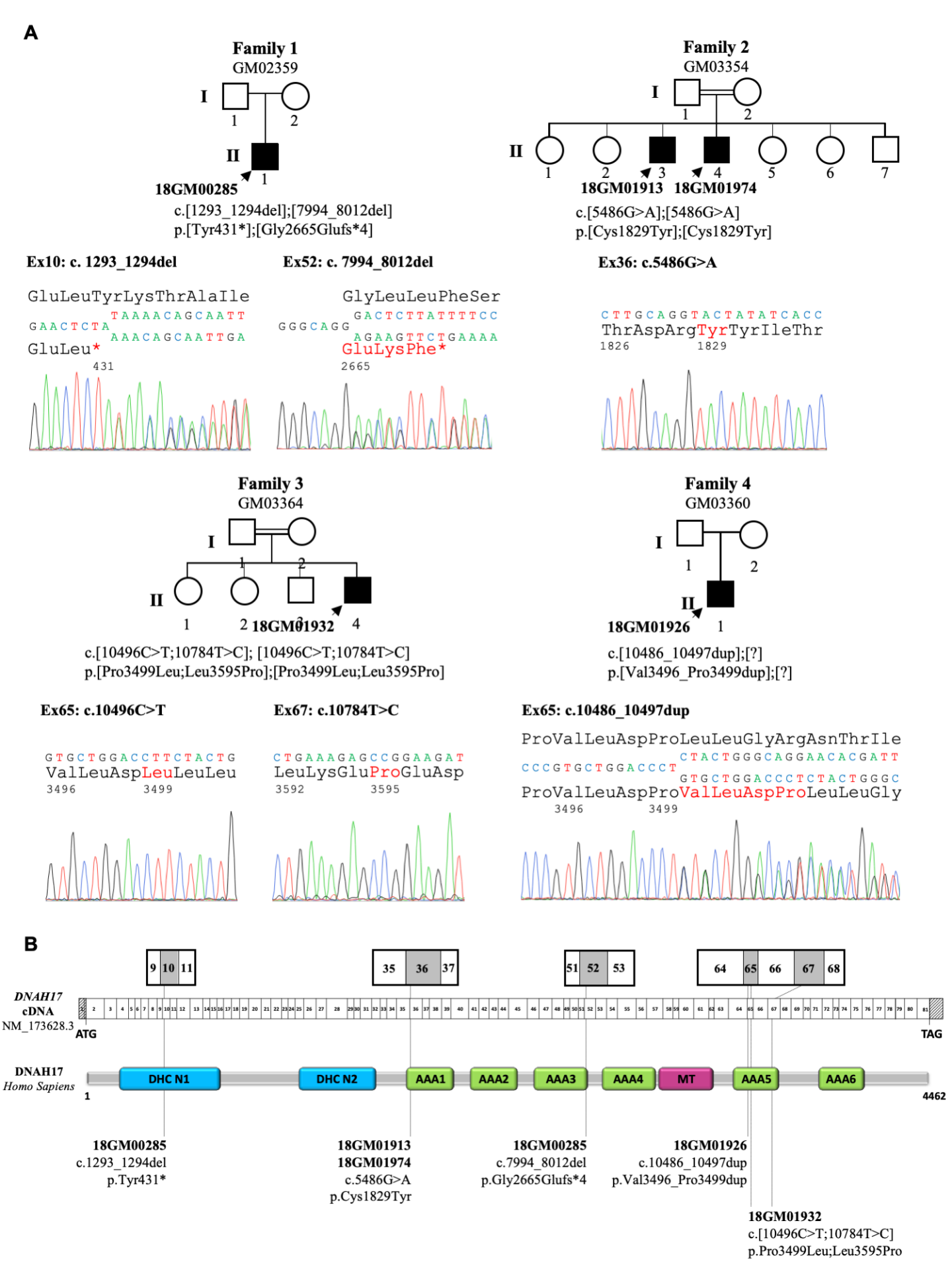
A
Family 1
GM02359
I
1
2
II
1
18GM00285
c.[1293_1294del];[7994_8012del]
p.[Tyr431*];[Gly2665Glufs*4]
Family 2
GM03354
I
1
2
II
1
2
3
4
5
6
7
18GM01913
18GM01974
c.[5486G>A];[5486G>A]
p.[Cys1829Tyr];[Cys1829Tyr]
Ex10: c. 1293_1294del
GluLeuTyrLysThrAlaIle
GAACTCTA TAAAACAGCAATT
AAACAGCAATTGA
GluLeu*
431
Ex52: c. 7994_8012del
GlyLeuLeuPheSer
GGGCAGG GACTCTTATTTTCC
AGAAGTTCTGAAAA
GluLysPhe*
2665
Ex36: c.5486G>A
CTTGCAGGTACTATATCACC
ThrAspArgTyrTyrIleThr
1826
1829
Family 3
GM03364
I
1
2
II
1
2
3
4
18GM01932
c.[10496C>T;10784T>C]; [10496C>T;10784T>C]
p.[Pro3499Leu;Leu3595Pro];[Pro3499Leu;Leu3595Pro]
Family 4
GM03360
I
1
2
II
1
18GM01926
c.[10486_10497dup];[?]
p.[Val3496_Pro3499dup];[?]
Ex65: c.10496C>T
GTGCTGGACCTTCTACTG
ValLeuAspLeuLeuLeu
3496
3499
Ex67: c.10784T>C
CTGAAAGAGCCGGAAGAT
LeuLysGluProGluAsp
3592
3595
Ex65: c.10486_10497dup
ProValLeuAspProLeuLeuGlyArgAsnThrIle
CCCGTGCTGGACCCT CTACTGGGCAGGAACACGATT
GTGCTGGACCCTCTACTGGGC
ProValLeuAspProValLeuAspProLeuLeuGly
3496
3499
B
9
10
11
35
36
37
51
52
53
64
65
66
67
68
DNAH17
cDNA
NM_173628.3
ATG
TAG
DNAH17
Homo Sapiens
DHC N1
DHC N2
AAA1
AAA2
AAA3
AAA4
MT
AAA5
AAA6
1
4462
18GM00285
c.1293_1294del
p.Tyr431*
18GM01913
18GM01974
c.5486G>A
p.Cys1829Tyr
18GM00285
c.7994_8012del
p.Gly2665Glufs*4
18GM01926
c.10486_10497dup
p.Val3496_Pro3499dup
18GM01932
c.[10496C>T;10784T>C]
p.Pro3499Leu;Leu3595Pro

Figure 4

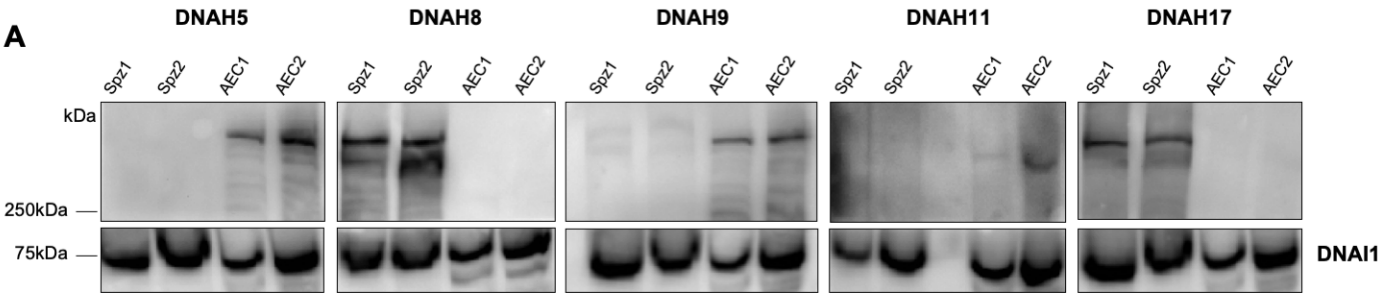
A
DNAH5
DNAH8
DNAH9
DNAH11
DNAH17
Spz1
Spz2
AEC1
AEC2
kDa
250kDa
75kDa
DNAI1

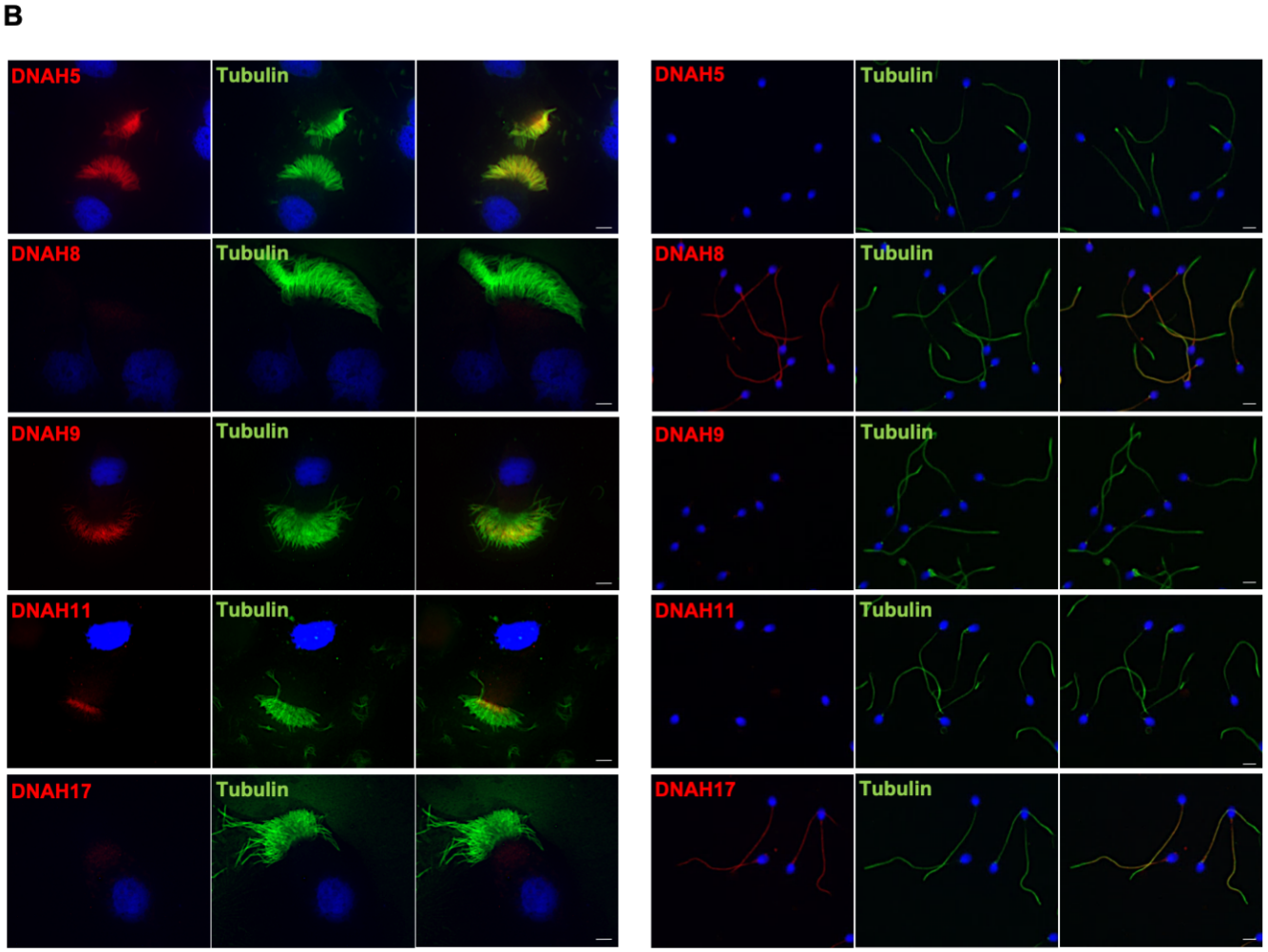
B
DNAH5
Tubulin
DNAH8
Tubulin
DNAH9
Tubulin
DNAH11
Tubulin
DNAH17
Tubulin
DNAH5
Tubulin
DNAH8
Tubulin
DNAH9
Tubulin
DNAH11
Tubulin
DNAH17
Tubulin

Figure 5

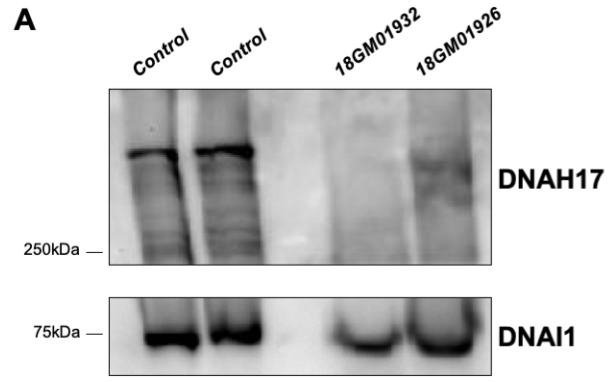
A
Control
Control
18GM01932
18GM01926
DNAH17
250kDa
75kDa
DNAI1

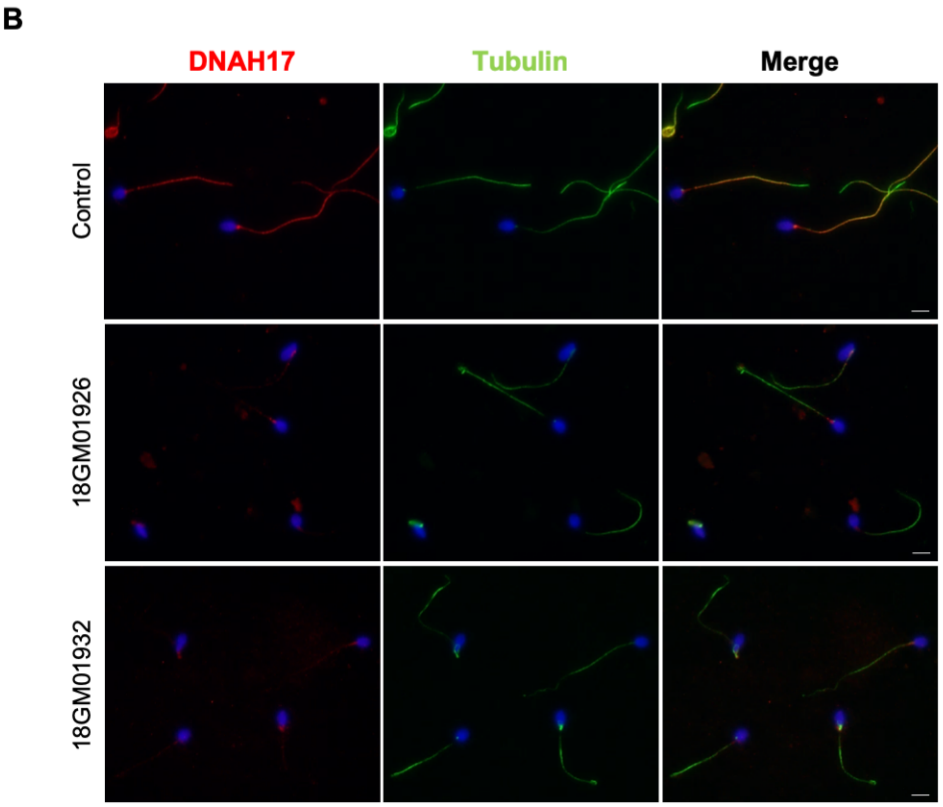
B
DNAH17
Tubulin
Merge
Control
18GM01926
18GM01932

Figure 6

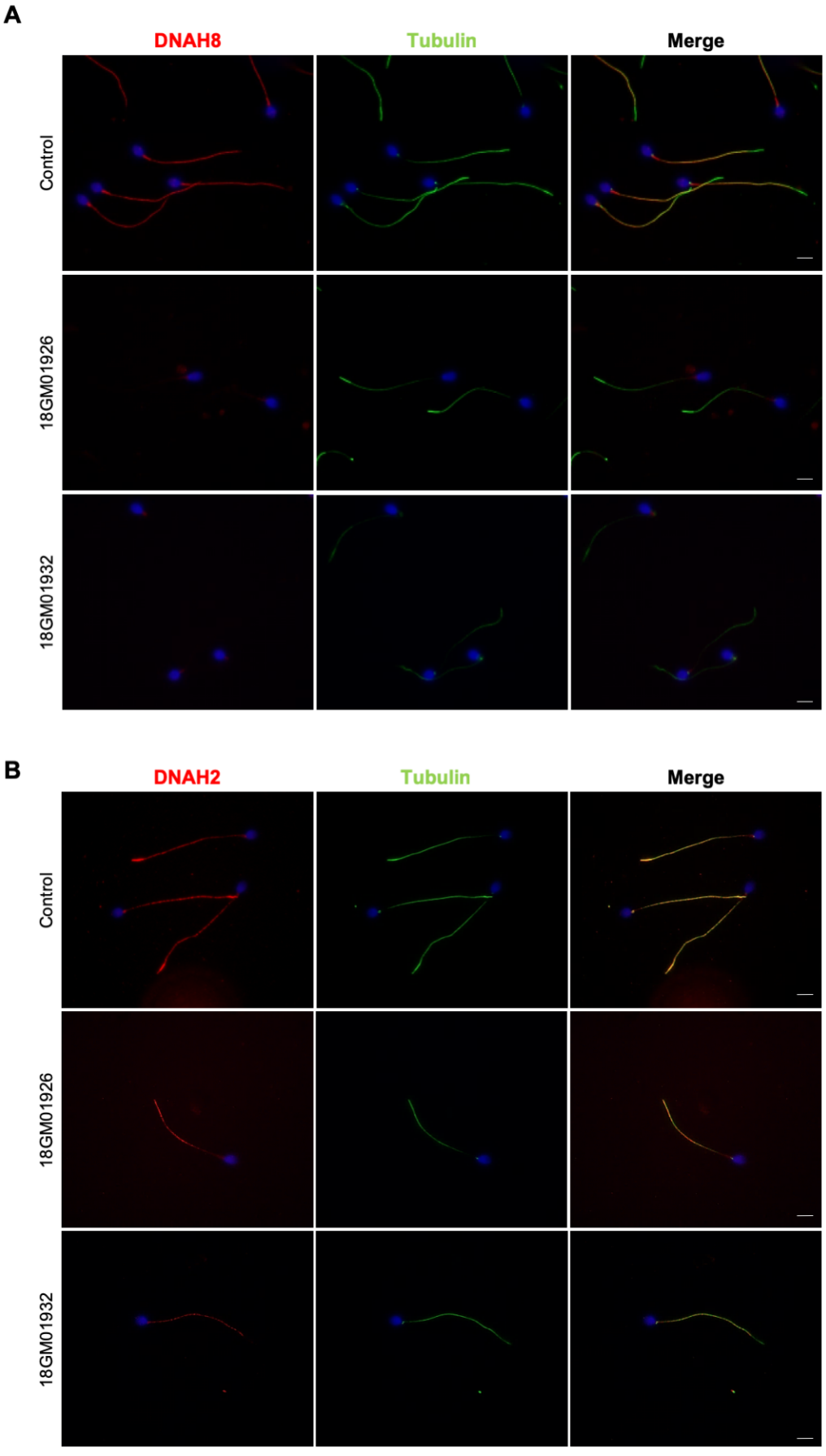
A
DNAH8
Tubulin
Merge
Control
18GM01926
18GM01932
B
DNAH2
Tubulin
Merge
Control
18GM01926
18GM01932

Figure 7

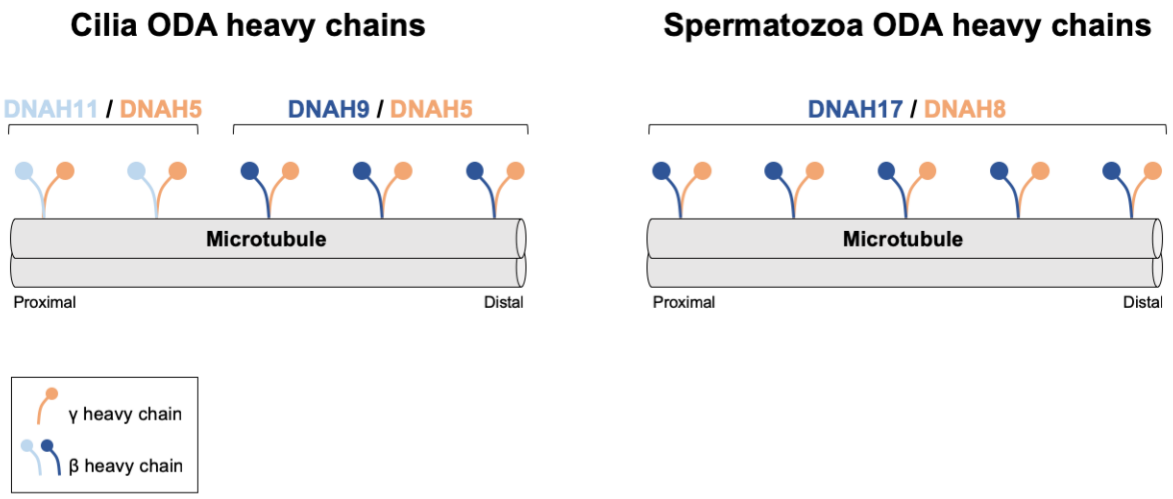
Cilia ODA heavy chains
DNAH11 / DNAH5
DNAH9 / DNAH5
Microtubule
Proximal
Distal
γ heavy chain
β heavy chain
Spermatozoa ODA heavy chains
DNAH17 / DNAH8
Microtubule
Proximal
Distal